tRNA-derived microRNA modulates proliferation and the DNA damage response and is down-regulated in B cell lymphoma

Roy L. Maute[a,b], Christof Schneider[a], Pavel Sumazin[a,c], Antony Holmes[a], Andrea Califano[a,c], Katia Basso[a,d,1,2], and Riccardo Dalla-Favera[a,b,d,e,1,2]

[a]Institute for Cancer Genetics and Herbert Irving Comprehensive Cancer Center, [b]Department of Genetics and Development, [c]Joint Centers for Systems Biology, [d]Department of Pathology and Cell Biology, and [e]Department of Microbiology and Immunology, Columbia University, New York, NY 10032

Sequencing studies from several model systems have suggested that diverse and abundant small RNAs may be derived from tRNA, but the function of these molecules remains undefined. Here, we demonstrate that one such tRNA-derived fragment, cloned from human mature B cells and designated CU1276, in fact possesses the functional characteristics of a microRNA, including a *DICER1*-dependent biogenesis, physical association with Argonaute proteins, and the ability to repress mRNA transcripts in a sequence-specific manner. Expression of CU1276 is abundant in normal germinal center B cells but absent in germinal center-derived lymphomas, suggesting a role in the pathogenesis of this disease. Furthermore, CU1276 represses endogenous *RPA1*, an essential gene involved in many aspects of DNA dynamics, and consequently, expression of this tRNA-derived microRNA in a lymphoma cell line suppresses proliferation and modulates the molecular response to DNA damage. These results establish that functionally active microRNAs can be derived from tRNA, thus defining a class of genetic entities with potentially important biological roles.

In recent decades, sequencing studies have uncovered a diverse menagerie of small RNA molecules expressed in eukaryotic cells, among which microRNAs (miRNAs) are perhaps the single best-understood subclass. miRNAs guide the binding of Argonaute-containing miRNA-induced silencing complexes (miRISC) to the 3′ untranslated region (3′UTR) of genes bearing partially complementary sites and are typically expressed from within the introns of protein coding genes or as part of long noncoding RNA transcripts (1). However, recent work has demonstrated that miRNAs can also arise from previously unanticipated non-canonical pathways. Specifically, miRNAs can be generated in a *DROSHA*- (2, 3) or *DICER1*-independent manner (4) and have been demonstrated to arise from cleavage of otherwise functional noncoding RNA molecules, such as small nucleolar RNA (5).

Previously, we reported cloning and sequencing of small RNAs purified from human naïve, germinal center (GC), and memory B cells, as well as from the Burkitt lymphoma cell line Ramos (6). In addition to observing previously reported miRNAs, we noted an intriguing class of abundantly expressed small RNAs whose sequences perfectly matched either to mature or to precursor tRNA transcripts. Several other groups have reported similar small RNA species expressed in a variety of human cell types (7–11) and in other organisms (12–14). However, the functional role of these small RNAs, and in particular the possibility that they may act as miRNAs, has not yet been adequately addressed. Here, we show that at least one such sequence, designated CU1276, functions as a miRNA.

Results

CU1276 Is a *DICER1*-Dependent tRNA Fragment Expressed in Mature B Cells.

Taken together, previous reports (8, 9, 11) define a minimum of three distinct categories of tRNA fragment: those matching to the 5′ end of mature tRNA (tRF-5), those matching to the 3′ end of mature tRNA (tRF-3), and those matching to the 3′ end of precursor tRNA transcripts (tRF-1). Further analysis of our published small RNA sequencing data (6) suggested that among these classes, tRF-3s are by far the most abundant variety expressed in mature B cells; therefore, to investigate the biological function of these molecules, we sought to characterize a representative sequence of the tRF-3 class, designated CU1276.

CU1276 is a 22-nt small RNA (5′-TCGATTCCCGGCCAA-TGCACCA-3′) differentially expressed in three stages of mature B-cell differentiation and one GC-derived lymphoma cell line, and cloned most frequently in normal GC B cells (Fig. 1A). Despite its miRNA-like size, CU1276 is a perfect match to the posttranscriptionally modified 3′ end of at least five annotated human tRNAs (15) (Fig. 1B). To clarify the relationship between CU1276 and tRNA, we cloned a CU1276-matching tRNA locus into an expression vector and transiently transfected this vector into HEK-293T cells (293T). Northern blot analysis of these cells revealed a clear increase in both the mature tRNA and a 22-nt band comigrating with the endogenous fragment observed in B cells (Fig. 1C), suggesting that CU1276 is tRNA derived. We also confirmed CU1276 expression from a second, independent Gly (GCC) tRNA locus and ruled out the possibility of expression from a candidate precursor genomic locus (6) closely matching the CU1276 sequence, but not encoding a tRNA (Fig. S1).

tRNA do not meet the structural criteria of a classical DICER1 substrate (16); nonetheless, because of the observed similarities in size between CU1276 and *DICER1*-dependent miRNA, we hypothesized that this enzyme could be involved in CU1276 biogenesis. Therefore, we transiently overexpressed a CU1276-matching tRNA in 293T cell lines stably expressing either a control shRNA or a pool of three *DICER1*-targeting shRNA. Northern blot analysis revealed that knockdown of DICER1 was sufficient to reduce production of CU1276, regardless of an accumulation of mature tRNA (Fig. 1D). This evidence strongly supports a *DICER1*-dependent cleavage step in the biogenesis of CU1276, which may be a general feature of fragments derived from mature tRNA.

CU1276 Associates with All Four Human Argonaute Proteins and Functions as a miRNA.

As a prerequisite for investigating a possible miRNA-like function of CU1276, we sought to determine whether this small RNA was physically associated with Argonaute
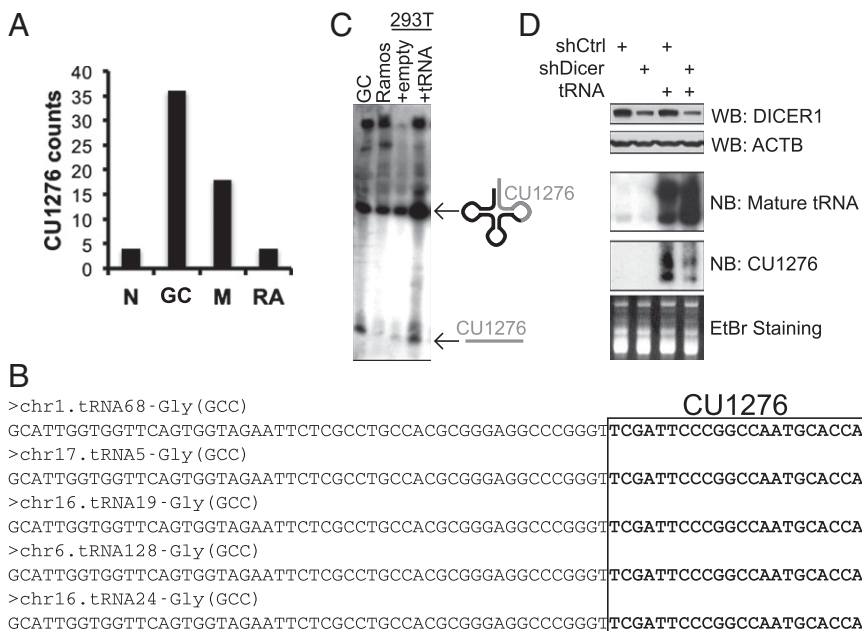
Fig. 1. CU1276 is a Dicer-dependent tRNA fragment expressed in mature B cells. (A) Cloning frequency of CU1276 from naïve (N), GC, and memory (M) B cells purified from human tonsil, and from the Burkitt's lymphoma cell line Ramos (RA). Data are derived from analysis of previously published small RNA libraries (6). (B) FASTA sequences of annotated human tRNAs with perfect match to the CU1276 small RNA. CU1276 sequence is highlighted in bold. (C) Northern blot analysis of total RNA from GC B cells, Ramos, and 293T cells transiently transfected with empty vector or a vector encoding for the Gly(GCC) chr1.tRNA68. The three primary bands correspond to the 22-nt tRNA fragment CU1276, the 74-nt mature tRNA, and a high molecular weight tRNA primary transcript. See also Fig. S1. (D) Western blot and Northern blot analyses of 293T cells stably expressing control shRNA (shCTRL) or a pool of three Dicer-targeting shRNA (shDicer), transiently transfected with empty or Gly(GCC) chr1.tRNA68 vector. Ethidium bromide (EtBr) staining and immunoblotting for ACTB were used as loading controls for Northern blot and Western blot, respectively.

proteins. Using a monoclonal antibody with reactivity against all four human Argonaute proteins (17), we purified Argonaute-associated RNAs from the B-cell line RIVA; quantitative RT-PCR (qRT-PCR) analysis of the coprecipitated RNA confirms that CU1276 is enriched in the pan-Ago immunoprecipitation (IP) fraction relative to a control IP (Fig. 2A). To dissect CU1276 binding affinity for each individual Argonaute protein, we performed IP of HA-tagged versions of human AGO1, AGO2, AGO3, and AGO4 transiently expressed in 293T cells; the results demonstrate that CU1276 is enriched in the IP fractions of each Argonaute protein relative to that of the HA-EGFP control, suggesting that it is specifically incorporated into silencing complexes containing each of the four human Argonautes (Fig. 2B). The dynamics of this interaction seem to be influenced by the availability of unoccupied Argonaute complexes, given that the magnitude of CU1276 enrichment in AGO1 complexes increased proportionally with the total levels of this protein, meeting and eventually exceeding the enrichment of the canonical miRNA miR-16 at high levels of AGO1 expression (Fig. 2C).

Given its demonstrated binding to the functional effectors of miRNA signaling, we tested the effect of CU1276 on a firefly luciferase reporter bearing two antisense binding sites in its 3′UTR. Because overexpression of full-length tRNA inevitably produces a complex mixture of RNA molecules, including a previously reported ~34-nt 5′ tRNA fragment capable of broadly repressing translation (18), we also cloned CU1276 into a miRNA hairpin to investigate its activity in a context free from confounding factors. Expression of either the tRNA or hairpin was sufficient to repress the antisense reporter (Fig. 2D). We noted that under standard conditions, the potency of tRNA-delivered CU1276 was less than that of hairpin-delivered CU1276; however, simultaneous expression of exogenous AGO2, the Argonaute family member whose slicer activity enables potent repression of mRNAs bearing a perfect antisense site (19), facilitated tRNA-mediated repression at comparable levels (Fig. 2D). Although these data are potentially consistent with a lower affinity for Argonaute proteins or a different distribution among Argonautes compared with canonical hairpin-derived miRNA, they nonetheless prove that the tRNA-derived CU1276 can repress mRNA targets in an Argonaute-dependent, miRNA-like fashion.

CU1276 Is Down-Regulated in Lymphoma Cell Lines and Primary Biopsies.

Formation of GC structures is a crucial step in the B-cell–mediated adaptive immune response, and GC cells are the cell of origin for the majority of B-cell lymphomas (20). Initial small RNA sequencing and Northern blot analysis suggested that CU1276 is abundantly expressed in normal GC B cells, but is low in at least one GC-derived lymphoma cell line (Fig. 1 A and C). To expand these findings, we assessed CU1276 by qRT-PCR in normal GC B cells and a panel of GC-derived lymphoma cell lines. Strikingly, only normal GC B cells efficiently expressed this small RNA, whereas the entire panel of cell lines displayed low CU1276 levels (Fig. 3A). Additionally, sequencing of small RNAs from a panel of normal GC B cells (n = 4) and diffuse large B cell lymphoma (DLBCL) primary biopsies (n = 25) revealed a binary pattern of CU1276 expression, with CU1276 almost completely absent in tumor cells (Fig. 3B).

Although the cause of this strong differential expression cannot be directly determined from this data, the Gly(GCC) tRNA from which CU1276 is derived can be found in at least five distinct genomic loci (Fig. 1B), making it an unlikely candidate for genetic deletion. Indeed, each cell line tested expresses roughly equal levels of the mature, posttranscriptionally modified form of the tRNA from which CU1276 is derived (Fig. S2), suggesting that the observed decrease in CU1276 production in lymphomas is probably regulated at the level of tRNA cleavage (Discussion).

CU1276 Represses a Set of Endogenous Genes, Including RPA1.

Based on a well-validated method for prediction of miRNA targets (21), we sought to identify genes both significantly down-regulated by CU1276 expression and computationally predicted to contain CU1276 binding sites in their 3′UTR. We anticipated that expression of mature Gly(GCC) tRNA was likely to induce changes in gene expression due to CU1276-independent effects on translation; therefore, to focus on the most physiologically relevant CU1276-specific targets, we compared expression profiles from 293T cells transfected with empty, tRNA-expressing, or CU1276 hairpin-expressing vectors. This analysis revealed a modest, but statistically significant overlap between the down-regulated probes (Student's t test, $P < 0.05$) in the two experimental groups (~13% of tRNA–down-regulated genes, and ~15% hairpin–down-regulated genes; hypergeometric test, $P < 1e\text{-}40$) (Fig. S3A), confirming that tRNA-delivered and hairpin-delivered
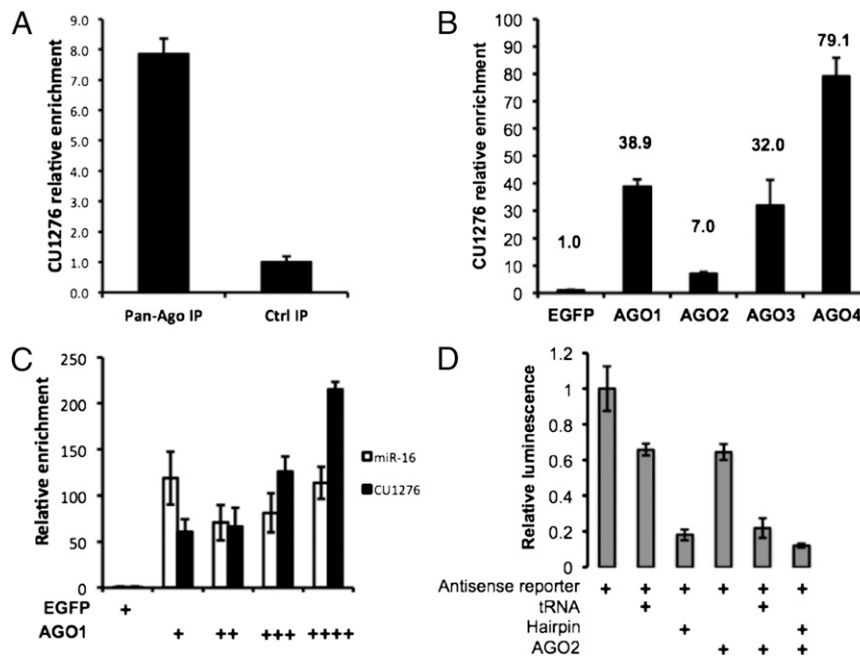
Fig. 2. CU1276 is bound by all four human Argonaute proteins and functions as a miRNA. qRT-PCR of CU1276 in pan-Ago and control immunoprecipitation (IP) fractions from RIVA cells (*A*), qRT-PCR of CU1276 in HA IP fractions from 293T cells transiently expressing equivalent levels of HA-tagged EGFP, AGO1, AGO2, AGO3, or AGO4 proteins (*B*), and qRT-PCR of miR-16 and CU1276 in IPs from 293T cells expressing HA-tagged EGFP, or increasing amounts of HA-tagged AGO1 (*C*). In all qRT-PCR graphs, values were normalized to 5s rRNA and plotted relative to control IP levels. Error bars represent the SD of triplicate qRT-PCRs. (*D*) Antisense 3′ UTR reporter activity in response to CU1276, with or without exogenous AGO2 expression. Firefly luciferase values were normalized to a Renilla luciferase control and plotted relative to reporter cotransfected with empty vector; error bars represent the SD of two independent experiments, each performed in duplicate.

CU1276 exert a similar effect on at least a subset of mRNA. Furthermore, transcripts predicted to contain CU1276 binding sites by the miRNA target prediction algorithm TargetScan (22) were significantly enriched (hypergeometric test, $P = 8.6e\text{-}8$) in the union of genes down-regulated by tRNA and/or hairpin expression (Fig. S3*B*), suggesting that a significant fraction of these genes are repressed based on classical seed-mediated binding.

To focus on the highest-confidence predictions, we narrowed our attention to those genes (*i*) significantly down-regulated in both tRNA- and in hairpin-expressing cells, (*ii*) predicted by TargetScan to contain CU1276 binding sites, and (*iii*) expressed in the physiological site of CU1276 expression, GC B cells. Three genes met these criteria, and all three were tested as targets for CU1276.

Two of these genes, *WHSC1L1* and *STAG2*, showed either no response, or an ambiguous response to CU1276 expression (Fig.

S3 *C* and *D*). In contrast, CU1276 expression via either tRNA or hairpin was sufficient to significantly (Student's *t* test, $P = 3.9e\text{-}5$ and $P = 8.2e\text{-}5$, respectively) repress a reporter bearing the 3′UTR of the *RPA1* gene (Fig. 4*A*). Mutation of the lone predicted CU1276 binding site rendered the reporter immune to this repression, confirming that the interaction is direct (Fig. 4*A*).

Consistent with this result, transient expression of CU1276 by either tRNA- or hairpin-mediated delivery repressed endogenous RPA1 protein in 293T cells while leaving another RPA complex member, RPA2, unchanged (Fig. 4*B* and Fig. S4*A*). CU1276 expression had minimal effect on *RPA1* mRNA levels as measured by qRT-PCR (Fig. S4*B*), suggesting that in this cellular context, CU1276-mediated repression of *RPA1* is primarily at the translational level. To extend this finding to B cells, we constructed a stable B-cell lymphoma line carrying a vector with
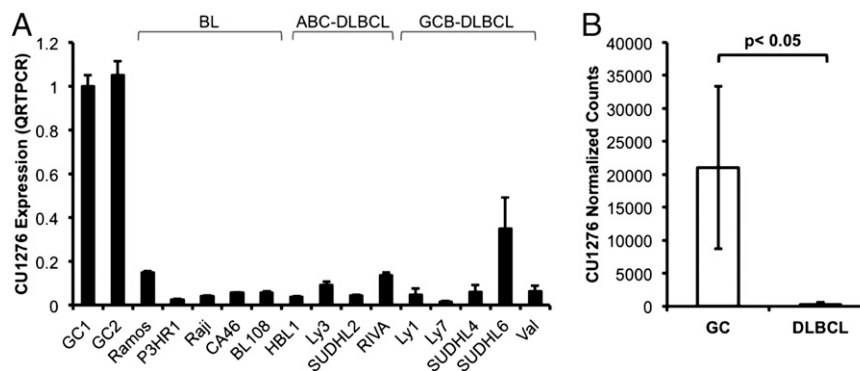
Fig. 3. CU1276 is down-regulated in lymphoma cell lines and primary biopsies. (*A*) qRT-PCR of CU1276 in GC samples and B-cell lymphoma lines, including Burkitt lymphoma (BL), activated B cell-like diffuse large B cell lymphoma (ABC-DLBCL), and GC-like diffuse large B cell lymphoma (GCB-DLBCL); qRT-PCR levels were normalized to RNU66 and graphed relative to GC1. Error bars represent the SD of triplicate PCR reactions (see also Fig. S2). (*B*) CU1276 counts from deep sequencing of small RNA libraries from purified GC ($n = 4$) and primary biopsies of DLBCL ($n = 25$). DLBCL includes ABC-DLBCL ($n = 13$) and GCB-DLBCL ($n = 12$) subtypes.

Fig. 4. CU1276 directly represses RPA1. (*A Upper*) Schematic representation of the region in the 3′UTR of RPA1 targeted by CU1276. The mutations introduced into this region are highlighted in gray. (*A Lower*) RPA1 3′UTR reporter activity in response to CU1276 expression. Firefly luciferase values were normalized to a Renilla luciferase control, and plotted relative to reporter cotransfected with empty vector; error bars represent the SD of seven independent experiments, each performed in duplicate. The reporter is significantly repressed by either Gly(GCC) chr1.tRNA68- (Student's *t* test, P = 3.9e-5) or hairpin-mediated delivery (Student's *t* test, P = 8.2e-5) of CU1276. (*B*) Western blot analyses of RPA1 and RPA2 from 293T cells transiently transfected with empty, Gly(GCC) chr1.tRNA68-expressing-, or CU1276 hairpin-expressing vector, and from stable lines of the Burkitt lymphoma cell line P3HR1 engineered to inducibly express GFP (empty) or GFP plus CU1276 (CU1276). GFP indicates successful doxycycline induction of vector. ACTB was used as loading control. Images are representative of four independent experiments each; see also Fig. S4. (*C*) Western blot analysis and graphical quantification of RPA1, RPA2, and DICER1, with ACTB used as loading control, from normal GC B cells and a panel of GC-derived lymphoma cell lines, including BL, activated B-cell-like diffuse large B cell lymphoma (ABC-DLBCL), and GCB-DLBCL. The GC sample was obtained by pooling cells from two independent donors. All samples are identical to those used for CU1276 expression analysis in Fig. 3A.

a doxycycline-inducible bidirectional promoter encoding for GFP alone, or GFP plus CU1276 hairpin; induction of CU1276 repressed both endogenous RPA1 protein and *RPA1* mRNA relative to control cells (Fig. 4B and Fig. S4 *C and D*). Thus, *RPA1* is a bona fide target of the tRNA-derived miRNA CU1276.

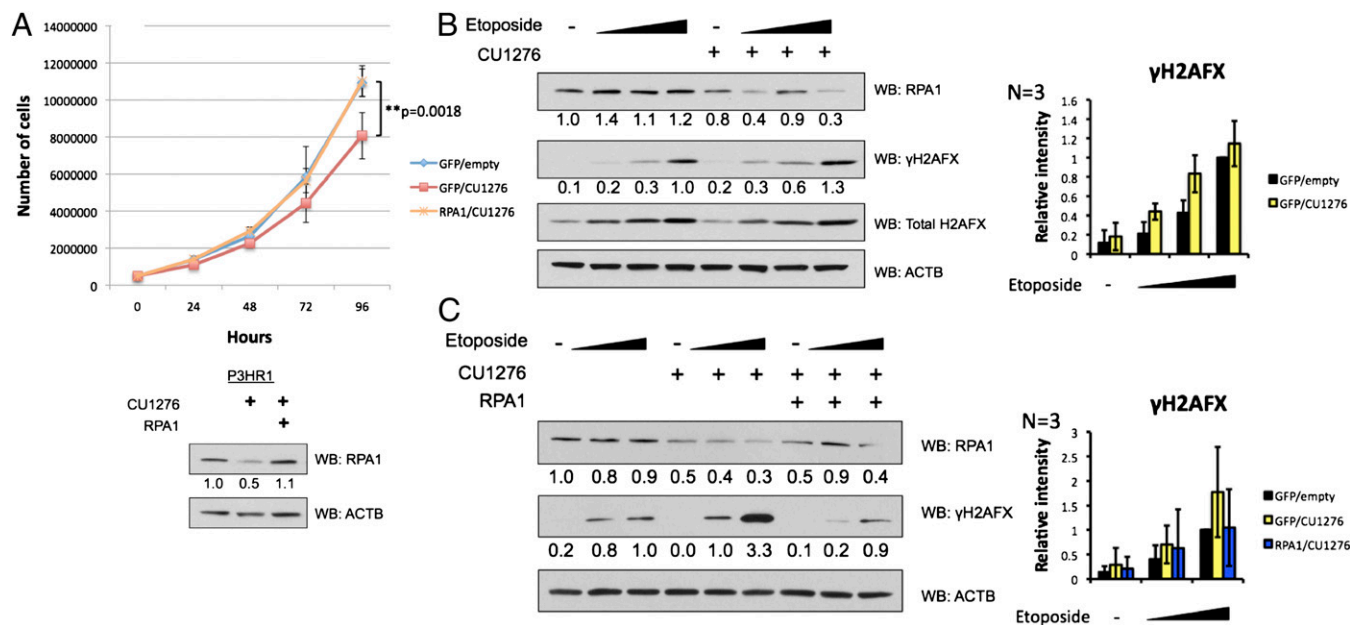Based on our observation of strongly differential CU1276 expression between normal GC B cells and GC-derived lymphomas (Fig. 3), we hypothesized that RPA1 protein might be derepressed in cell types lacking CU1276. Consistent with this hypothesis, the majority of tested cell lines express higher levels of RPA1 relative to normal GC B cells (Fig. 4C). *RPA1* mRNA levels, as evaluated by gene expression profiling in an independent panel of five GC samples and a subset of eight DLBCL cell lines, were similar between these two groups, consistent with a translational-level regulatory effect by CU1276 (Fig. S5). Although sufficient material was not available to directly assess RPA1 protein levels in the primary lymphoma biopsies, based on the high levels of expression observed in cell lines, we speculate that loss of CU1276 expression may also contribute to misregulation of *RPA1* in the context of primary lymphomas.

CU1276 Suppresses Proliferation and Modulates the Molecular Response to DNA Damage in an *RPA1*-Dependent Manner. *RPA1* has a number of well-characterized roles in DNA dynamics, including in replication and DNA repair (23). We therefore hypothesized that

through repression of *RPA1*, CU1276 might influence cellular proliferation and the response to DNA damage.

Indeed, stable expression of CU1276 in a Burkitt lymphoma cell line modestly but significantly reduces the proliferation rate of these cells (Student's *t* test, P = 1.8e-3; Fig. 5A), consistent with defective DNA replication efficiency. Critically, restoration of RPA1 protein expression to wild-type levels through simultaneous coexpression of exogenous *RPA1* significantly rescues the observed growth impairment (Fig. 5A), confirming that *RPA1* is the primary CU1276 target responsible for this phenotype.

In addition to its effect on cellular proliferation, CU1276 expression is also capable of modulating the molecular response to DNA damage. Robust expression of CU1276 is sufficient to sensitize a Burkitt lymphoma cell line to etoposide-induced DNA damage, as measured by an increase in H2AFX phosphorylation relative to controls (Fig. 5B). Similar to the CU1276-induced reduction in cellular proliferation, this sensitization can be fully rescued by restoration of RPA1 protein to wild-type levels (Fig. 5C), confirming that *RPA1* is also the critical CU1276 target responsible for this effect.

Discussion

An increasing body of literature supports the existence of highly abundant miRNA-like tRNA fragments in a variety of cell types (7–14), but despite several lines of speculation, no conclusive evidence of their function has yet been shown. Our data demonstrates

Fig. 5. CU1276 modulates proliferation and DNA damage signaling in an RPA1-dependent manner. Growth curves of P3HR1 stable cell lines containing bidirectional, doxycycline-inducible vectors expressing GFP alone (blue line), GFP plus the CU1276 hairpin (red line), or *RPA1* plus the CU1276 hairpin (orange line) (*A Upper*), and corresponding Western blot analysis of RPA1 protein levels from these cell lines, with ACTB used as loading control (*A Lower*). Growth curve data are compiled from eight independent experiments, with each genotype represented by four independently derived bulk populations. Error bars represent the 95% confidence intervals of each cell type, calculated according to a normal distribution. CU1276 expression is sufficient to significantly reduce cellular proliferation relative to the GFP control at 96 h (Student's *t* test, *P = 1.8e-3). At 96 h, *RPA1* rescue restores growth completely to wild-type levels. (*B*) Western blot analysis of RPA1, total H2AFX, and γH2AFX in etoposide-treated control cells and cells expressing CU1276. ACTB was used as loading control. Image is representative of three independent experiments, for which average γH2AFX quantifications are indicated in bar chart format. Error bars represent the SD of three independent experiments. (*C*) Western blot analysis of control cells, cells expressing CU1276, and cells simultaneously expressing CU1276 and exogenous *RPA1*. Restoration of RPA1 protein levels rescues CU1276-mediated sensitization of H2AFX phosphorylation upon etoposide treatment. ACTB was used as loading control. Image is representative of three independent experiments, for which average γH2AFX quantifications are indicated in bar chart format. Error bars represent SDs.

that despite its derivation from the 3′ end of a mature tRNA (Fig. 1*C*), the small RNA CU1276 has all of the structural and functional characteristics of a miRNA, including a *DICER1*-dependent biogenesis (Fig. 1*D*) and binding to all four human Argonaute proteins (Fig. 2 *A* and *B*). CU1276 is furthermore capable of guiding repression to both artificial antisense sites (Fig. 2*D*) and binding sites identified in endogenous 3′UTRs (Fig. 4 *A* and *B*).

In addition to their classical role in delivering amino acids to nascent peptide chains, tRNAs and tRNA fragments have the capacity to regulate a surprising range of cellular processes, including translational efficiency under stress conditions (18), mitochondrial-mediated apoptosis (24), and oncogenic transformation (25). The data presented here further extend the regulatory repertoire of tRNA, and greatly expand the pool of candidate miRNAs, by demonstrating that a tRNA fragment can posttranscriptionally regulate endogenous genes in a sequence-specific, miRNA-like fashion.

Interestingly, we observe that the tRNA-derived microRNA CU1276 is strongly down-regulated in GC-derived lymphomas relative to their cell of origin (Fig. 3). Given that mature Gly (GCC) tRNA expression is largely constant between samples with highly discordant CU1276 levels (Fig. S2 and Fig. 3*A*), the defect in CU1276 biogenesis is likely to lie at the level of *DICER1* cleavage. However, with only one exception (HBL1), all tested lymphoma cell lines express abundant DICER1 protein (Fig. 4*C*), suggesting that a more complex mode of regulation, such as differences in posttranscriptional modifications that might protect the tRNA from processing (26), is likely to be responsible for the observed differences. Further investigation of the factors regulating CU1276 biogenesis will help to shed light on the upstream cause of this repression in cancer cells, whereas

validation of additional CU1276 targets will help to clarify its full downstream biological consequences.

As proof of principle for its ability to regulate endogenous target genes, we have demonstrated that CU1276 represses endogenous *RPA1* (Fig. 4 *A* and *B*). *RPA1* is an essential gene for many aspects of DNA dynamics, including genome replication. Consequently, stable CU1276 expression in a Burkitt lymphoma-derived cell line results in an RPA1-dependent suppression of their proliferation rate (Fig. 5*A*). This result, combined with the observed down-regulation of CU1276 levels in lymphoma cell lines and biopsies (Fig. 3) suggests that loss of CU1276 expression, and a corresponding increase in RPA1 protein levels, may confer a growth advantage to malignant cells.

As part of their maturation, GC B cells undergo several physiological processes of somatic mutation and DNA rearrangement (20). *RPA1* is a required component for some types of DNA repair and additionally has a GC-specific role in facilitating *AICDA*-mediated mutagenic processes (27, 28). Physiological expression of CU1276 in the GC may contribute to fine-tuning of *RPA1* levels in GC B cells and may thereby indirectly influence the efficiency of DNA repair, somatic hypermutation, and class-switch recombination. Consistent with such a role, CU1276 expression in a Burkitt lymphoma-derived cell line results in an *RPA1*-dependent sensitization of the molecular response of these cells to DNA damage, as indicated by phosphorylation of H2AFX upon etoposide treatment (Fig. 5 *B* and *C*). Thus, our observations suggest that the tRNA-derived miRNA CU1276 may be a genetic participant in the modulation of DNA damage response pathways in the GC. Furthermore, loss of CU1276 expression in lymphomas may decrease their sensitivity to ongoing

DNA damage, thereby helping them to tolerate the accumulation of mutations and genomic aberrations during tumor evolution.

Much remains to be elucidated regarding the biogenesis and function of CU1276 and similar tRF molecules, but the validation of CU1276 as a miRNA establishes a clear regulatory potential for a large fraction of the abundant tRNA fragments expressed in many cell types. Further investigation may reveal that many additional tRNA fragments also act as miRNA, with potentially far-reaching biological consequences.

Materials and Methods

Cell Culture and Transfection. The 293T cells were maintained in DMEM supplemented with 10% (vol/vol) FBS and 1% Penicillin/Streptomycin. All B-cell lines were maintained in IMDM supplemented with 10% (vol/vol) FBS and 1% Penicillin/Streptomycin. Transfection of 293T cells was achieved by standard calcium phosphate precipitation, or by PEI-based transfection, as described (29). The 293T-shCtrl and 293T-shDICER stable cell lines were established by transfection with pLKO-based vectors (see *SI Materials and Methods* for details of plasmids and cloning information) followed by selection for 4 d with 2 μg/mL puromycin. P3HR1 stable cells were established by electroporation of exponentially growing cells with 5 pmol of pRTS1-GLSVP-based vectors according to standard protocol. After a 48-h recovery in IMDM supplemented with 20% (vol/vol) FBS, cells were selected with 0.5 μg/mL puromycin for 4 d. Induction of expression from stable P3HR1 cells was achieved by addition of doxycycline to growth media at a concentration of 100 ng/mL DNA damage response of stable P3HR1 cell lines was assayed by preinduction with doxycycline for 24 h, followed by treatment with 0 μM, 1 μM, 2 μM, or 10 μM concentrations of etoposide (Sigma) for 3 h.

Northern Blot and qRT-PCR. Total RNA was purified with TRIzol Reagent (Invitrogen) according to manufacturer's indications. Northern blot was performed as described (6), using 30 μg of total RNA from each sample. Prehybridization, hybridization, and washing were performed at 55 °C. For CU1276 and tRNA detection, 5′-TGGTGCATTGGCCGGG-3′ probe was [γ-^{32}P]ATP labeled by polynucleotide kinase (Fermentas). Images were obtained by exposure to film for 24–48 h. qRT-PCR was also performed as described (6), starting from 2 μg of total RNA or a percentage of RNA from IP fraction. qRT-PCR analysis of cDNA was performed with ABsolute Blue Sybr Green Master Mix (Thermo Scientific) by using an AB7300 thermocycler (Applied Biosystems).

Western Blot and 3′UTR Reporter Assay. Cell pellets were lysed in RIPA buffer followed by 10 min of sonication, cleared of debris by centrifugation, and then quantified with Bradford Reagent (BioRad). Fifth micrograms of protein lysate was run on precast Tris-Glycine gradient gels (Novex), transferred to Hybond ECL membrane (GE Healthcare), and subjected to standard immunoblotting technique. Antibody information, incubation conditions, and quantification procedures are indicated in *SI Materials and Methods*. For 3′UTR reporter assays, firefly and renilla luciferase activities were assayed according to standard protocol by using the Dual Luciferase Reporter Assay System (Promega) and measured on a Lumat LB 9507 luminometer (Berthold Technologies).

Argonaute Immunoprecipitation. Argonaute immunoprecipitation was performed as described (17), starting from 1×10^8 exponentially growing RIVA cells or ~5×10^7 293T cells, with anti–pan-AGO antibody (MABE56; Millipore), or control IgG overnight with rotation at 4 °C. Protein G magnetic beads (New England Biosciences) were added to lysates, and the mixture was incubated for 3 h with rotation at 4 °C. HA-tagged proteins were immunoprecipitated by overnight incubation of lysate with EZ view HA affinity beads (Sigma). Beads were washed and resuspended in TRIzol Reagent (Invitrogen) or lysis buffer for downstream RNA and protein analysis, respectively.

Gene Expression Profiling and Data Analysis. Gene expression profiles were generated from total RNA by using the HG-U133Plus2.0 platform (Affymetrix) according to the manufacturer's indications. Differential expression was determined by Student's t test using the geWorkbench software suite (30), with a significance cutoff of $P < 0.05$.

Generation and Sequencing of Small RNA Libraries. GC B cells were isolated from tonsil tissue by magnetic cell sorting as reported (31). Tonsil tissue was collected at the Columbia-Presbyterian Medical Center by following approval by the institutional ethical committee. DLBCL primary biopsies were excess from diagnostic tissue frozen at the time of diagnosis. Total RNA was isolated by TRIzol Reagent (Invitrogen), and the small RNA fraction was enriched by flashPAGE fractionation (Ambion). Small RNA libraries were generated by using the SOLiD Small RNA Expression Kit (Applied Biosystems), following the manufacturer's indications. SOLiD sequencing was performed on 4 libraries of purified GC B cells and 25 libraries of DLBCL. After removal of artifacts and rRNA fragments SOLiD sequences were subject to a previously developed pipeline to identify candidate miRNAs (6), whereas tRNA-derived fragments were detected by alignment to the UCSC tRNA database (15). Normalized small RNA counts were obtained by correcting for the size of each library.

1. He L, Hannon GJ (2004) MicroRNAs: Small RNAs with a big role in gene regulation. *Nat Rev Genet* 5(7):522–531.
2. Bogerd HP, et al. (2010) A mammalian herpesvirus uses noncanonical expression and processing mechanisms to generate viral MicroRNAs. *Mol Cell* 37(1):135–142.
3. Ruby JG, Jan CH, Bartel DP (2007) Intronic microRNA precursors that bypass Drosha processing. *Nature* 448(7149):83–86.
4. Cheloufi S, Dos Santos CO, Chong MM, Hannon GJ (2010) A dicer-independent miRNA biogenesis pathway that requires Ago catalysis. *Nature* 465(7298):584–589.
5. Ender C, et al. (2008) A human snoRNA with microRNA-like functions. *Mol Cell* 32(4):519–528.
6. Basso K, et al. (2009) Identification of the human mature B cell miRNome. *Immunity* 30(5):744–752.
7. Burroughs A, et al. (2011) Deep-sequencing of human argonaute-associated small RNAs provides insight inot miRNA sorting and reveals argonaute association with RNA fragments of diverse origin. *RNA Biol* 8(1):20.
8. Cole C, et al. (2009) Filtering of deep sequencing data reveals the existence of abundant Dicer-dependent small RNAs derived from tRNAs. *RNA* 15(12):2147–2160.
9. Haussecker D, et al. (2010) Human tRNA-derived small RNAs in the global regulation of RNA silencing. *RNA* 16(4):673–695.
10. Kawaji H, et al. (2008) Hidden layers of human small RNAs. *BMC Genomics* 9:157.
11. Lee YS, Shibata Y, Malhotra A, Dutta A (2009) A novel class of small RNAs: tRNA-derived RNA fragments (tRFs). *Genes Dev* 23(22):2639–2649.
12. Babiarz JE, Ruby JG, Wang Y, Bartel DP, Blelloch R (2008) Mouse ES cells express endogenous shRNAs, siRNAs, and other Microprocessor-independent, Dicer-dependent small RNAs. *Genes Dev* 22(20):2773–2785.
13. Couvillion MT, Sachidanandam R, Collins K (2010) A growth-essential Tetrahymena Piwi protein carries tRNA fragment cargo. *Genes Dev* 24(24):2742–2747.
14. Hsieh LC, et al. (2009) Uncovering small RNA-mediated responses to phosphate deficiency in Arabidopsis by deep sequencing. *Plant Physiol* 151(4):2120–2132.
15. Chan PP, Lowe TM (2009) GtRNAdb: A database of transfer RNA genes detected in genomic sequence. *Nucleic Acids Res* 37(Database issue):D93–D97.
16. Hammond SM (2005) Dicing and slicing: The core machinery of the RNA interference pathway. *FEBS Lett* 579(26):5822–5829.
17. Nelson PT, et al. (2007) A novel monoclonal antibody against human Argonaute proteins reveals unexpected characteristics of miRNAs in human blood cells. *RNA* 13(10):1787–1792.
18. Ivanov P, Emara MM, Villen J, Gygi SP, Anderson P (2011) Angiogenin-induced tRNA fragments inhibit translation initiation. *Mol Cell* 43(4):613–623.
19. Liu J, et al. (2004) Argonaute2 is the catalytic engine of mammalian RNAi. *Science* 305(5689):1437–1441.
20. Klein U, Dalla-Favera R (2008) Germinal centres: Role in B-cell physiology and malignancy. *Nat Rev Immunol* 8(1):22–33.
21. Lim LP, et al. (2005) Microarray analysis shows that some microRNAs downregulate large numbers of target mRNAs. *Nature* 433(17):5.
22. Lewis BP, Burge CB, Bartel DP (2005) Conserved seed pairing, often flanked by adenosines, indicates that thousands of human genes are microRNA targets. *Cell* 120(1):15–20.
23. Haring SJ, Mason AC, Binz SK, Wold MS (2008) Cellular functions of human RPA1. Multiple roles of domains in replication, repair, and checkpoints. *J Biol Chem* 283(27):19095–19111.
24. Mei Y, et al. (2010) tRNA binds to cytochrome c and inhibits caspase activation. *Mol Cell* 37(5):668–678.
25. Marshall L, Kenneth NS, White RJ (2008) Elevated tRNA(iMet) synthesis can drive cell proliferation and oncogenic transformation. *Cell* 133(1):78–89.
26. Blanco S, et al. (2011) The RNA-methyltransferase Misu (NSun2) poises epidermal stem cells to differentiate. *PLoS Genet* 7(12):e1002403.
27. Chaudhuri J, Khuong C, Alt FW (2004) Replication protein A interacts with AID to promote deamination of somatic hypermutation targets. *Nature* 430(7003):992–998.
28. Yamane A, et al. (2011) Deep-sequencing identification of the genomic targets of the cytidine deaminase AID and its cofactor RPA in B lymphocytes. *Nat Immunol* 12(1):62–69.
29. Ehrhardt C, et al. (2006) Polyethylenimine, a cost-effective transfection reagent. *Signal Transduct* 6(3):179–184.
30. Floratos A, Smith K, Ji Z, Watkinson J, Califano A (2010) geWorkbench: An open source platform for integrative genomics. *Bioinformatics* 26(14):1.
31. Klein U, et al. (2003) Transcriptional analysis of the B cell germinal center reaction. *Proc Natl Acad Sci USA* 100(5):2639–2644.

GENETICS